Measurement of the Radiative K_{e3} Branching Ratio

NA48 Collaboration

A. Lai, D. Marras

Dipartimento di Fisica dell'Università e Sezione dell'INFN di Cagliari,
I-09100 Cagliari, Italy

A. Bevan, R.S. Dosanjh, T.J. Gershon, B. Hay, G.E. Kalmus,
C. Lazzeroni, D.J. Munday, E. Olaiya[2], M.A. Parker,
T.O. White, S.A. Wotton

Cavendish Laboratory, University of Cambridge, Cambridge, CB3 0HE, U.K.[1]

G. Barr, G. Bocquet, A. Ceccucci, T. Cuhadar-Dönszelmann,
D. Cundy[3], G. D'Agostini, N. Doble[4], V. Falaleev,
L. Gatignon, A. Gonidec, B. Gorini, G. Govi, P. Grafström,
W. Kubischta, A. Lacourt, A. Norton, S. Palestini,
B. Panzer-Steindel, H. Taureg, M. Velasco[5], H. Wahl[6]

CERN, CH-1211 Genève 23, Switzerland

C. Cheshkov[7], P. Hristov[7], V. Kekelidze, L. Litov[7],
D. Madigojine, N. Molokanova, Yu. Potrebenikov, S. Stoynev,
A. Zinchenko

Joint Institute for Nuclear Research, Dubna, 141980, Russian Federation

I. Knowles, V. Martin[5], R. Sacco[9], A. Walker

Department of Physics and Astronomy, University of Edinburgh, JCMB King's
Buildings, Mayfield Road, Edinburgh, EH9 3JZ, U.K.

M. Contalbrigo, P. Dalpiaz, J. Duclos, P.L. Frabetti[10],
A. Gianoli, M. Martini, F. Petrucci, M. Savrié

Dipartimento di Fisica dell'Università e Sezione dell'INFN di Ferrara,
I-44100 Ferrara, Italy

A. Bizzeti [11], M. Calvetti, G. Collazuol [4], G. Graziani [12],
E. Iacopini, M. Lenti, F. Martelli [13], M. Veltri [13]

Dipartimento di Fisica dell'Università e Sezione dell'INFN di Firenze,
I-50125 Firenze, Italy

H.G. Becker, K. Eppard, M. Eppard [7], H. Fox [5], A. Kalter,
K. Kleinknecht, U. Koch, L. Köpke, P. Lopes da Silva,
P. Marouelli, I. Pellmann [15], A. Peters [7], B. Renk, S.A. Schmidt,
V. Schönharting, Y. Schué, R. Wanke, A. Winhart,
M. Wittgen [16]

Institut für Physik, Universität Mainz, D-55099 Mainz, Germany [14]

J.C. Chollet, L. Fayard, L. Iconomidou-Fayard, J. Ocariz,
G. Unal, I. Wingerter-Seez

Laboratoire de l'Accélérateur Linéaire, IN2P3-CNRS,Université de Paris-Sud,
91898 Orsay, France [17]

G. Anzivino, P. Cenci, E. Imbergamo, P. Lubrano,
A. Mestvirishvili, A. Nappi, M. Pepe, M. Piccini

Dipartimento di Fisica dell'Università e Sezione dell'INFN di Perugia,
I-06100 Perugia, Italy

L. Bertanza, R. Carosi, R. Casali, C. Cerri, M. Cirilli [7],
F. Costantini, R. Fantechi, S. Giudici, I. Mannelli,
G. Pierazzini, M. Sozzi

Dipartimento di Fisica, Scuola Normale Superiore e Sezione dell'INFN di Pisa,
I-56100 Pisa, Italy

J.B. Cheze, J. Cogan, M. De Beer, P. Debu, A. Formica,
R. Granier de Cassagnac, E. Mazzucato, B. Peyaud, R. Turlay,
B. Vallage

DSM/DAPNIA - CEA Saclay, F-91191 Gif-sur-Yvette, France

M. Holder, A. Maier, M. Ziolkowski

Fachbereich Physik, Universität Siegen, D-57068 Siegen, Germany [18]

R. Arcidiacono, C. Biino, N. Cartiglia, F. Marchetto,
E. Menichetti, N. Pastrone

*Dipartimento di Fisica Sperimentale dell'Università e Sezione dell'INFN di
Torino, I-10125 Torino, Italy*

J. Nassalski, E. Rondio, M. Szleper[5], W. Wislicki, S. Wronka

*Soltan Institute for Nuclear Studies, Laboratory for High Energy Physics,
PL-00-681 Warsaw, Poland*[19]

H. Dibon, G. Fischer, M. Jeitler, M. Markytan, I. Mikulec,
G. Neuhofer, M. Pernicka, A. Taurok, L. Widhalm

*Österreichische Akademie der Wissenschaften, Institut für Hochenergiephysik,
A-1050 Wien, Austria*[20]

Abstract.

We present a measurement of the relative branching ratio of the decay $K^0 \to \pi^\pm e^\mp \nu \gamma$ ($K_{e3\gamma}$) with respect to $K^0 \to \pi^\pm e^\mp \nu$ (γ) ($K_{e3} + K_{e3\gamma}$) decay. The result is based on observation of 19 000 $K_{e3\gamma}$ and $5.6 \cdot 10^6$ K_{e3} decays. The value of the branching ratio is $Br(K^0_{e3\gamma}, E^*_\gamma > 30 \text{ MeV}, \theta^*_{e\gamma} > 20^o)/Br(K^0_{e3}) = (0.964 \pm 0.008^{+0.011}_{-0.009})\%$. This result agrees with theoretical predictions but is at variance with a recently published result.

1 Introduction

The study of radiative K_L decays can give valuable information on the kaon structure. It allows a good test of theories describing hadron interactions and decays, like Chiral Perturbation Theory (ChPT). Here we present a study of the radiative K_{e3} decay.

There are two distinct photon components in the radiative K^0_{e3} decays - inner bremsstrahlung (IB) and direct emission. K^0_{e3} decays are mainly sensitive to the IB component because of the small electron mass m_e. A big contribution to the rate, dominated by the IB amplitude, comes from the region of small photon energies E^*_γ and angles $\theta^*_{e\gamma}$ between the charged lepton and the photon, with both E^*_γ and $\theta^*_{e\gamma}$ measured in the kaon rest frame. $K^0_{e3\gamma}$ amplitude has infrared singularity at $E^*_\gamma \to 0$, and a collinear singularity at $\theta^*_{e\gamma} \to 0$ when $m_e = 0$. For this measurement and the corresponding theoretical evaluation, we exclude these regions by the restriction $E^*_\gamma > 30$ MeV and $\theta^*_{e\gamma} > 20^o$.

Two different theoretical approaches for evaluation of the branching ratio have been used. Current algebra technique together with the Low theorem were applied by Fearing, Fischbach and Smith (called FFS hereafter) [1],[2] and by Doncel [3]. ChPT calculations were performed in [4], [5] and are being continuously improved [6], [7]. The ratio of the $K^0_{e3\gamma}$ to K^0_{e3} decay probabilities, applying the standard cuts on E^*_γ and $\theta^*_{e\gamma}$, is predicted to be between 0.95 and 0.99%. The amounts of direct emission in these various calculations differ, and are roughly estimated to be between 0.1 and 1 % of the size of the IB component.

Two experimental measurements of the $K^0_{e3\gamma}$ branching ratio have been published. The NA31 experiment obtained $Br(K^0_{e3\gamma}, E^*_\gamma > 30 \text{ MeV}, \theta^*_{e\gamma} > 20^o)/Br(K^0_{e3}) = (0.934 \pm 0.036^{+0.055}_{-0.039})\%$ [8]. The KTeV experiment gave a compatible value of the ratio $Br(K^0_{e3\gamma}, E^*_\gamma > 30 \text{ MeV}, \theta^*_{e\gamma} > 20^o)/Br(K^0_{e3}) = (0.908 \pm 0.008^{+0.013}_{-0.012})\%$ [9]. However, this value does not agree well with theoretical predictions.

2 Experimental setup

The NA48 detector was designed for a measurement of direct CP violation in the K^0 system. Here we use data from a dedicated run in September 1999 where a K_L beam was produced by 450 GeV/c protons from the CERN SPS incident on a beryllium target. The decay region is located 120 m from the K_L target after three collimators and sweeping magnets. It is contained in an evacuated tube, 90 m long, terminated by a thin ($3 \cdot 10^{-3} X_0$) kevlar window.

The detector components relevant for this measurement include the following:

The **magnetic spectrometer** is designed to measure the momentum of charged particles with high precision. The momentum resolution is given by

$$\frac{\sigma(p)}{p} = (0.48 \oplus 0.009 \cdot p)\,\% \tag{1}$$

where p is in GeV/c. The spectrometer consists of four drift chambers (DCH), each with 8 planes of sense wires oriented along the projections x,u,y,v, each one rotated by 45 degrees with respect to the previous one. The spatial resolution achieved per projection is 100 μm and the time resolution is 0.7 ns. The volume between the chambers is filled with helium, near atmospheric pressure. The spectrometer magnet is a dipole with a field integral of 0.85 Tm and is placed after the first two chambers. The distance between the first and last chamber is 21.8 m.

The **hodoscope** is placed downstream of the last drift chamber. It consists of two planes of scintillators segmented in horizontal and vertical strips and arranged in four quadrants. The signals are used for a fast coincidence of two charged particles in the trigger. The time resolution from the hodoscope is 200 ps per track.

The **electromagnetic calorimeter** (LKr) is a quasi-homogeneous calorimeter based on liquid krypton, with tower read out. The 13212 read-out cells have cross sections of 2 x 2 cm^2. The electrodes extend from the front to the back of the detector in a small angle accordion geometry. The LKr calorimeter measures the energies of the $e^\pm$ and γ quanta by gathering the ionization from their electromagnetic showers. The energy resolution is :

$$\frac{\sigma(E)}{E} = \left(\frac{3.2}{\sqrt{E}} \oplus \frac{9.0}{E} \oplus 0.42 \right)\,\% \tag{2}$$

where E is in GeV, and the time resolution for showers with energy between 3 GeV and 100 GeV is 500 ps.

The **muon veto system** (MUV) consists of three planes of scintillator counters, shielded by iron walls of 80 cm thickness. It is used to reduce the $K_L \to \pi^\pm \mu^\mp \nu$ background.

Charged decays were triggered with a two-level trigger system. The trigger requirements were two charged particles in the scintillator hodoscope or in the drift chambers coming from the vertex in the decay region.

A more detailed description of the NA48 setup can be found elsewhere [10].

3   Analysis

3.1   Event selection

The data sample consisted of about 2 TB of data from 100 million triggers, with approximately equal amounts recorded with alternating spectrometer magnet polarities. These data are the same which were used for the measurement of the K_{e3} branching ratio [11]. The following selection criteria were applied to the reconstructed data to identify K_{e3} decays and to reject background, keeping in mind the main backgrounds to K_{e3}, which are $K_L \to \pi^\pm \mu^\mp \nu$ ($K_{\mu 3}$) and $K_L \to \pi^+ \pi^- \pi^0$ ($K_{3\pi}$):

- Each event was required to contain exactly two tracks, of opposite charge, and a reconstructed vertex in the decay region. To form a vertex, the closest distance of approach between these tracks had to be less than 3 cm. The decay region was defined by requirements that the vertex had to be between 6 and 34 m from the end of the last collimator and that the transverse distance between the vertex and the beam axis had to be less than 2 cm. These cuts were passed by 35 million events.

- The time difference between the tracks was required to be less than 6 ns. To reject muons, only events with both tracks inside the detector acceptance and without in-time hits in the MUV system were used. For the same reason only particles with a momentum larger than 10 GeV were accepted. In order to allow a clear separation of pion and electron showers, we required the distance between the entry points of the two tracks at the front face of the LKr Calorimeter to be larger than 25 cm. As a result 14 million events remained.

- For the identification of electrons and pions, we used the ratio of the measured cluster energy, E, in the LKr calorimeter associated to a track to the momentum, p, of this track as measured in the magnetic spectrometer. The ratio E/p for a sample of 75 000 pion tracks, selected by requiring the other track of a 2-track event to be an electron with $E/p > 1.02$, is shown in fig. 1. As a cross-check pion samples from $K_{2\pi}$ and $K_{3\pi}$ decays were selected giving similar results. Also shown in the figure is the distribution for 450 000 electron tracks which are selected from 2-track events where the other track is a pion, with $0.4 < E/p < 0.6$. For the selection of K_{e3} events, we require one track to have $0.93 < E/p < 1.10$ (electron) and the other track to have $E/p < 0.90$ (pion). 11.7 million events were accepted.
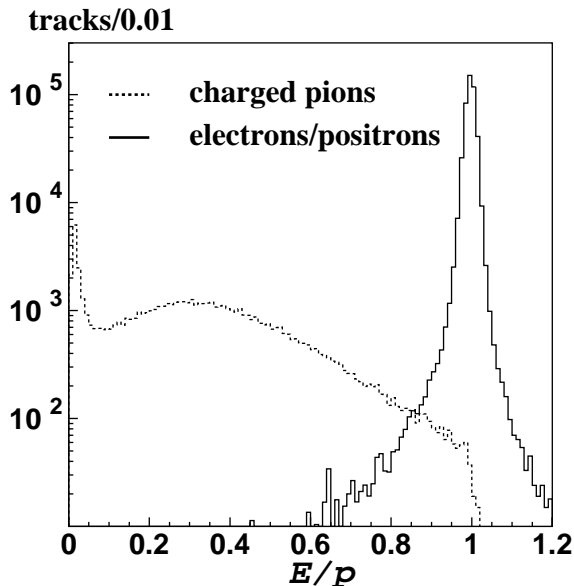
Fig. 1. Distribution of the ratio of the shower energy E reconstructed by the LKr and the momentum p reconstructed by the spectrometer, for pions (dotted) and electrons (line) from K_{e3} events (see text).

- In order to reduce background from $K_{3\pi}$ decays, we required the quantity

$$P_0'^2 = \frac{(m_K^2 - m_{+-}^2 - m_{\pi^0}^2)^2 - 4(m_{+-}^2 m_{\pi^0}^2 + m_K^2 p_\perp^2)}{4(p_\perp^2 + m_{+-}^2)} \tag{3}$$

to be less than $-0.004(\text{GeV/c})^2$. In the equation above, $p_\perp$ is the transverse momentum of the two track system (assumed to consist of two charged pions) relative to the K_L^0 flight direction and m_{+-}

is the invariant mass of the charged system. The variable $P_0'^2$ is positively defined if the charged particles are pions from the decay $K_{3\pi}$ and its distribution has maximum at zero. The cut removes $(98.94 \pm 0.03)\%$ of $K_{3\pi}$ decays and $(1.03 \pm 0.02)\%$ of K_{e3} decays as estimated with the Monte Carlo simulation (sect. 3.3). After this cut, we were left with 11.4 million K_{e3} candidate events.

The neutrino momentum in K_{e3} decays is not known and the kinematic reconstruction of the kaon momentum from the measured track momenta leads to a two-fold ambiguity in the reconstructed kaon momentum. The solution with larger energy we call "first solution". In order to measure the kaon momentum spectrum, we selected events in which both solutions for the kaon momentum lie in the same bin of width 8 GeV. These $4 \cdot 10^5$ events we call "diagonal events".

The last selection criterion was the requirement that each of the two solutions for the kaon energy had to be in the energy range (60,180) GeV. As a result of this selection, $5.6 \cdot 10^6$ fully reconstructed K_{e3} events were selected from the total sample. These selected events include radiative K_{e3} events.

For the selection of $K_{e3\gamma}$ events, the following additional requirements were made:

The distance between the γ cluster and the pion track in LKr had to be larger than 55 cm in order to allow a clear separation of the γ cluster from pion clusters. As is shown in fig. 2 the hadron showers can extend over lateral distances of up to 60 cm from the track entry point in LKr. After the requirements for $E_\gamma^* > 30$ MeV and $\theta_{e\gamma}^* > 20^o$ (for both solutions of the kaon energy),
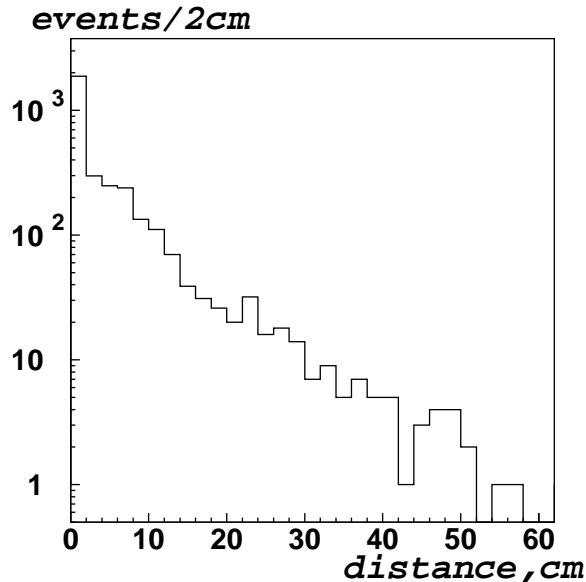

Fig. 2. Transverse distance between the pion entry point in LKr and the position of a cluster induced by pion interactions with matter; the pions here are selected from $K_L^0 \to \pi^+\pi^-$ decays where the entry points of the two tracks in the LKr calorimeter are at least 80 cm from each other; clusters have a minimum energy of 4 GeV

22 100 events survived. To distinguish the γ from the electron cluster we required the transverse distance between the γ cluster candidate and the electron track in LKr to be greater than 6 cm. The electromagnetic transverse rms shower width in LKr is 2.2 cm. An event was rejected if the γ cluster candidate was less than 16 cm away from the beam axis, because of the beam hole in the LKr calorimeter. We also rejected events with a γ cluster candidate with energy below 4 GeV because the energy resolution deteriorates below this threshold. Finally an event was rejected if

the γ was not in-time (more than 6 ns time difference) with the associated cluster(s). These cuts provided a sample of 19 117 $K_{e3\gamma}$ candidates.

3.2   Backgrounds

The amount of background was evaluated using a Monte Carlo simulation for other kaon decays.

The background to $K_{e3\gamma}$ events is small and comes from three sources - $K_{3\pi}$ and $K_L \rightarrow \pi^0 \pi^\pm e^\mp \nu$ (K_{e4}) decays as well as K_{e3} decays with an accidental photon. The $K_{3\pi}$ background was reduced by the cut on the variable $P_0'^2$ and the electron identification through the $E/p > 0.93$ condition. Variations of these cuts have a negligible effect, since the probability to misidentify a pion for an electron is only 0.57% from fig. 1, and the $P_0'^2$ distribution is well reproduced by the MC simulation. The estimated number of background events was 40^{+60}_{-40} events.

The K_{e4} background was evaluated to be 80 ± 40 events from the measured branching ratio and the calculated acceptance for these decays.

The contamination from K_{e3} decays with an accidental photon was estimated using the distribution of the time difference between the γ cluster candidate and the (average) time of the other cluster(s). The number of events in the two control regions $(-25, -10)$ ns and $(10, 25)$ ns were extrapolated to the signal region $(-6, 6)$ ns. The final number for this source of background was estimated to be 20^{+40}_{-20} events, assuming a flat distribution.

All backgrounds to $K_{e3\gamma}$ add up to 140 ± 82 events or 0.7% of the total $K_{e3\gamma}$ sample of 19117 events.

The main background to the normalization channel K_{e3} arises from $K_{3\pi}$ and $K_{\mu3}$ decays. The estimations were made as in the case of $K_{e3\gamma}$. All the background decays together gave a K_{e3} signature in less than $9 \cdot 10^{-5}$ of the cases (< 500 events). This percentage is negligible compared to background sources in $K_{e3\gamma}$ decay.

3.3   Monte Carlo Simulation

In order to calculate the geometrical and kinematical acceptance of the NA48 detector, a GEANT-based simulation was employed [10]. The kaon momentum spectrum from sect. 3.1 was implemented into the MC code. The radiative corrections (virtual and real) were taken into account by modifying the PHOTOS [12] program package in such a way as to reproduce the experimental data. This was achieved by weighting the angular distribution $\theta^*_{e\gamma}$ in the centre-of-mass frame such as to fit the experimental data (model independent analysis). With this procedure the MC and experimental data showed good agreement. As an example, the distributions of the neutrino energy, γ energy and $\theta^*_{e\gamma}$ (first solutions) in the centre-of-mass frame are presented in figures 3, 4, and 5 respectively. The upper plots of the figures show the experimental data distributions and the lower show the ratio of the data and the MC spectra, normalized to unity. The plots represent data with the negative magnet polarity and after the $K_{e3\gamma}$ selection.

The MC data were treated exactly in the same way as the experimental data and were used for

events/0.0045 GeV

slope: 0.44 ± 0.33 / GeV
χ^2**/ndf: 34.22 / 35**
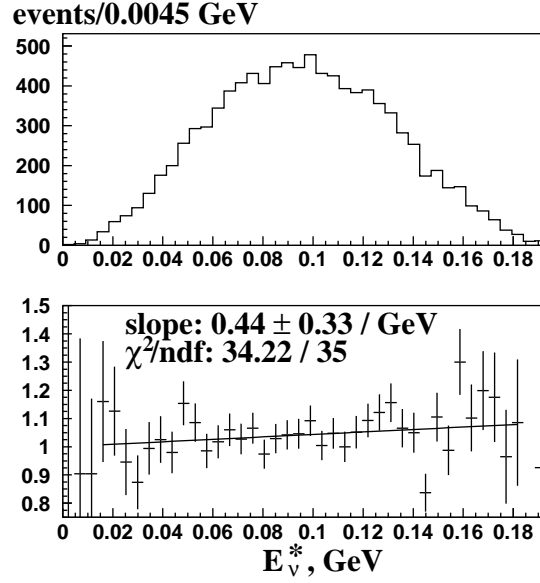
$\mathbf{E^*_\nu}$**, GeV**

Fig. 3. Reconstructed neutrino energy in the Center of Mass System; upper part - experimental data distribution, lower part - normalized to unity ratio of DATA/MC linearly fitted
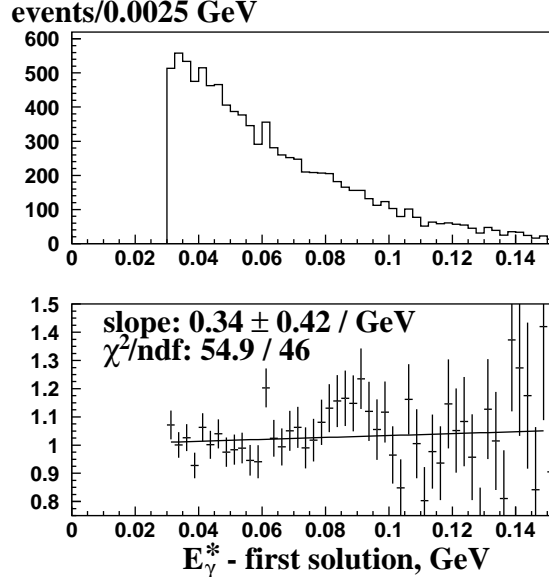
events/0.0025 GeV

slope: 0.34 ± 0.42 / GeV
χ^2**/ndf: 54.9 / 46**

$\mathbf{E^*_\gamma}$ **- first solution, GeV**

Fig. 4. First solution for E^*_γ; upper part - experimental data distribution, lower part - normalized to unity ratio of DATA/MC linearly fitted

acceptance calculations. The acceptance for $K_{e3\gamma}$ is $\epsilon(K_{e3\gamma}) = (6.08 \pm 0.03)\%$ as compared to the K_{e3} acceptance $\epsilon(K_{e3}) = (17.28 \pm 0.01)\%$.

3.4 Reconstruction and analysis technique

We used the "diagonal events" to measure the kaon momentum spectrum from K_{e3} decays. However, as this reduces the data sample significantly, for the analysis of the branching ratio the problem
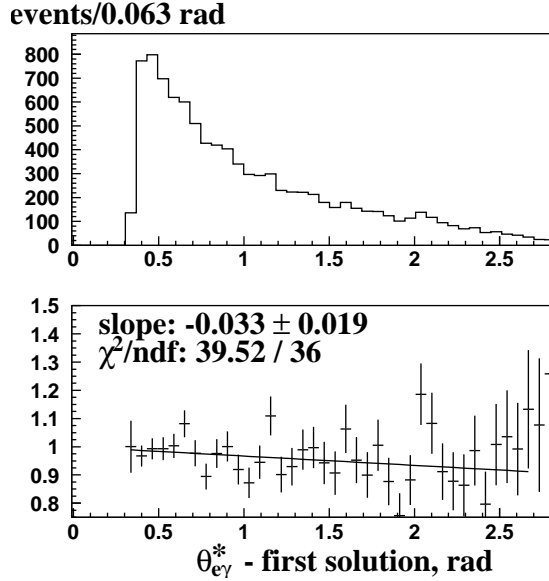
events/0.063 rad

Fig. 5. First solution for $\theta^*_{e\gamma}$; upper part - experimental data distribution, lower part - normalized to unity ratio of DATA/MC linearly fitted

was dealt with in another way. In the K_{e3} selection it was required that both solutions were in the range (60,180) GeV. Further in the $K_{e3\gamma}$ selection events were rejected if (at least) one of the two solutions for E^*_γ was less than 30 MeV or (at least) one of the two solutions for $\theta^*_{e\gamma}$ was less than 20°. The same procedure was used for selecting MC events when calculating the acceptance.

An important issue are radiative corrections. Only the inclusive rate ($K_{e3\gamma}$ plus any number of radiative photons) is finite and calculable. In our selection we have required only one hard γ satisfying $E^*_\gamma > 30$ MeV and $\theta^*_{e\gamma} > 20^o$. In this way in the final selection events with one "hard" γ and any number soft photons are included. Events with two or more hard photons are rejected. This loss has to be taken into account by MC in the calculation of the corresponding acceptance. In order to check the MC we have compared the number of γ clusters in the LKr calorimeter predicted by the MC with the one in the experimental data. A slight difference has been observed leading to a small correction of 0.05% to the branching ratio. We take this into account by a correction factor $C_M = 0.9995$ to the branching ratio. Additionally we have reanalysed our data, requiring at least one hard photon i.e. accepting any number of photons. This is the inclusive rate which is finite and can be calculated. The result for R agreed within 0.2% with the analysis requiring exactly one hard photon.

The trigger efficiency was measured to be $(98.1 \pm 0.1)\%$ for K_{e3} decays and $(98.1 \pm 0.6)\%$ for $K_{e3\gamma}$ decays.

On the basis of 19117 $K_{e3\gamma}$ candidates with an estimated background of 140 ± 82 events and 5.594 million K_{e3} events (including additional photons) after background subtraction, and using the calculated acceptances, the branching ratio was computed from the relation:

$$R = Br(K^0_{e3\gamma}, E^*_\gamma > 30 \text{ MeV}, \theta^*_{e\gamma} > 20^o)/Br(K^0_{e3}) = \frac{N(K_{e3\gamma})Acc(K_{e3})}{N(K_{e3})Acc(K_{e3\gamma})} \cdot C_M \qquad (4)$$

The result from 9361 $K_{e3\gamma}$ events and 2.728 million K_{e3} events for positive magnet polarity was
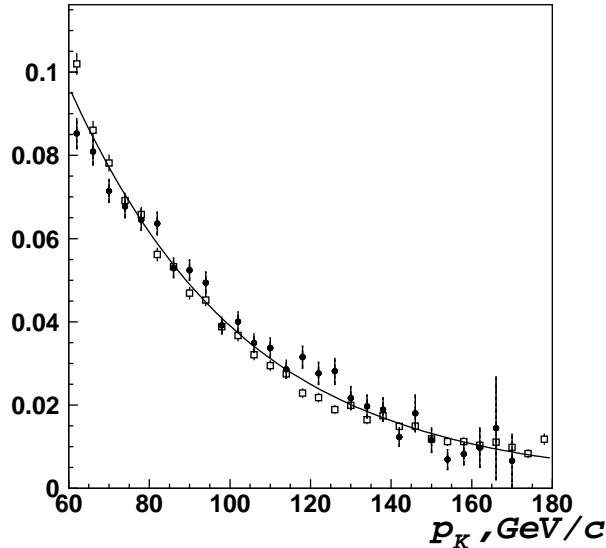
10

Fig. 6. Kaon momentum distribution obtained from K_{e3} (line), $K_{2\pi}$ (open squares) and $K_{3\pi}$ (circles) decays. Arbitrary units on Y-axis

$R = (0.953 \pm 0.010)\%$ and from 9616 $K_{e3\gamma}$ events and 2.866 million K_{e3} events for negative polarity, $R = (0.975 \pm 0.010)\%$, where the errors are statistical. We now turn to the systematic uncertainties.

3.5   Systematic uncertainties

Our investigation of possible systematic errors showed that the biggest uncertainty comes from the kaon momentum spectrum. In order to determine the influence of this factor we reconstructed the experimental kaon momentum distribution from $K \rightarrow \pi^+\pi^-$ and $K \rightarrow \pi^+\pi^-\pi^0$ decays and implemented them in the MC simulation. The shape of the spectrum for the three decays is shown in fig. 6. The systematic error from the momentum spectrum was estimated by taking the 3 different momentum spectra and calculating the effect of this variation on the acceptance ratio of K_{e3} and $K_{e3\gamma}$. It resulted in an relative uncertainty of $\left(\begin{smallmatrix} +6 \\ -3 \end{smallmatrix} \right) \cdot 10^{-3}$.

The stability of the result upon the various cuts used in the $K_{e3\gamma}$ selection was also investigated. The cuts were varied in between values which rejected no more than 10% of the events. The biggest fluctuations in the branching ratio estimation were taken as systematic errors, and all the errors were added in quadrature with a relative result of $\pm 5 \cdot 10^{-3}$.

Uncertainties in accidental photon events and in other background contributions are dominated by statistics and are not amongst the largest of the systematic errors $\left(\left(\begin{smallmatrix} +2 \\ -1 \end{smallmatrix} \right) \cdot 10^{-3} \text{ and } \left(\begin{smallmatrix} +4 \\ -3 \end{smallmatrix} \right) \cdot 10^{-3} \right.$ correspondingly). The influence of the K_{e3} selection cuts to the final result was estimated as in the case of $K_{e3\gamma}$ selection cuts. The quadratic addition of all these relative errors from variations of individual selection cuts yielded an inclusive relative error of $\pm 5 \cdot 10^{-3}$. The value of the form-factor λ_+ in the K_{e3} decay was varied between 0.019 and 0.029. The largest fluctuation was taken as a relative systematic error - $\pm 1 \cdot 10^{-3}$.

Our estimate of the systematic errors is summarized in Table 1.

11

Source	$\triangle R/R$
K_L spectrum	$^{+6}_{-3} \cdot 10^{-3}$
$K_{e3\gamma}$ selection	$\pm 5 \cdot 10^{-3}$
γ accidentals	$^{+2}_{-1} \cdot 10^{-3}$
Background uncertainties	$^{+4}_{-3} \cdot 10^{-3}$
K_{e3} selection	$\pm 5 \cdot 10^{-3}$
Form-factor uncertainties	$\pm 1 \cdot 10^{-3}$
TOTAL	$^{+11}_{-\ 9} \cdot 10^{-3}$

Table 1
Relative systematic uncertainties to the Branching ratio

4 Results and conclusion

The results are based on 18977 $K_{e3\gamma}$ and $5.594 \cdot 10^6$ K_{e3} events. We obtain the following value for the branching ratio including the systematic error:

$$R = (0.964 \pm 0.008^{+0.011}_{-0.009})\,\% = (0.964^{+0.014}_{-0.012})\,\% \tag{5}$$

Figure 7 shows this branching ratio compared to theoretical and experimental results. The authors of ref. [7] have undertaken a serious effort to estimate the theoretical uncertainties in R, while for the earlier theoretical values, this error is not known. These authors obtain $R = (0.96 \pm 0.01)\,\%$. It appears that our experimental result agrees well with the theoretical calculations [2], [3], including the most recent one [7]. However our result is at variance with a recent experiment with similar statistical sensitivity [9]. Our measurement, with a 1.5% precision, therefore confirms the validity of calculations based on chiral perturbation theory.
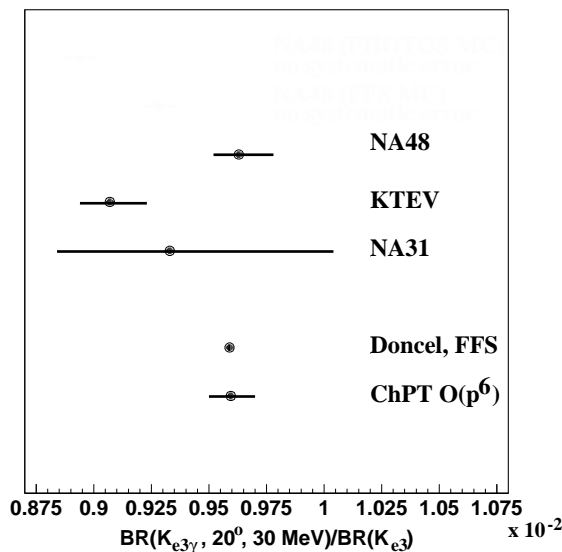

Fig. 7. Theoretical and experimental results for the radiative K_{e3} branching ratio. The two lower entries in the plot are theoretical results.

5 Acknowledgement

We would like to thank Drs. Jüerg Gasser, Bastian Kubis and Nello Paver for fruitful discussions and for communicating to us their result in ref.[7] prior to publication. We also thank the technical staff of the participating institutes and computing centres for their continuing support.

References

[1] H. Fearing et al., Phys. Rev. Lett. 24, (1970)189.

[2] H. Fearing et al., Phys. Rev. D 2, (1970)542.

[3] M. G. Doncel, Phys. Lett. 32B, (1970)623.

[4] B.R.Holstein, Phys. Rev. D 41, (1990)2829.

[5] J. Bijnens et al., Nucl. Phys. B369, (1993)81.

[6] V.Cirigliano et al., Eur.Phys.J. C23, (2002)121.
     V.Cirigliano et al., Eur.Phys.J. C35, (2004)53.
     J. Bijnens and P. Talavera, Nucl. Phys. B669, (2003)341.

[7] J. Gasser, B. Kubis, N. Paver, M. Verbeni, in preparation.

[8] F.Leber et al., Phys. Lett. B369, (1996)69.

[9] A. Alavi-Harati et al., The KTeV Collaboration, Phys. Rev. D 64, (2001)112004.

[10] A.Lai et al., The NA48 Collaboration, Eur. Phys. J. C 22, (2001)231.

[11] A.Lai et al., Preprint CERN-PH-EP/2004-47, hep-ex/0410059, submitted to Phys. Lett. B.

[12] E. Barberio and Z. Was, Comp. Phys. Comm. 79, (1994)291.